

Polarisation of CdF₂ by blocking electrodes. II. The effect of passing currents

This article has been downloaded from IOPscience. Please scroll down to see the full text article.

1989 J. Phys.: Condens. Matter 1 2087

(<http://iopscience.iop.org/0953-8984/1/11/017>)

View [the table of contents for this issue](#), or go to the [journal homepage](#) for more

Download details:

IP Address: 171.66.16.90

The article was downloaded on 10/05/2010 at 18:00

Please note that [terms and conditions apply](#).

Polarisation of CdF_2 by blocking electrodes: II. The effect of passing currents†

A Kessler

Institut für Theoretische Physik, University of Stuttgart, 7000 Stuttgart, PO Box 801140,
Federal Republic of Germany

Received 28 June 1988

Abstract. Thermally stimulated depolarisation (TSD) currents and charging and discharging currents at room temperature were obtained with graphite-contacted CdF_2 . The results and scrutiny of published TSD data show that, besides the known impurity-complex and point-defect space-charge polarisation, the currents are caused by charge carriers 'trapped' at Cd colloids segregated below the contact surface and by the electrochemical potential which Cd and accumulated fluorine entail.

1. Introduction

The fact that ionic crystals are 'polarised' by the passage of a current is notorious and was known long before solid-state physics as such came into being. There are a variety of effects which suggest this: the decay with time of the current caused by a constant voltage; the current of opposite sign, which also decays with time, obtained when a crystal is shorted after the passage of a current; a non-linear voltage-current (V - A) characteristic; a non-linear potential distribution in the crystal; capacitive and resistive AC effects; etc. In general only little is known about the cause(s) of these effects and the term 'polarisation' is in this connection a general name: it may, but need not, be identical with 'dielectric polarisation'. The phenomena are of both theoretical and practical interest: theoretical because polarisation is obviously closely connected with surface properties, solid-state 'reactions', etc; practical because of the strong impact on the electrical properties of crystals whether measured or employed in some device.

Investigations of the polarisation of contacted crystals by means of thermally stimulated depolarisation (TSD) measurements have shown that the relaxation of the polarisation is governed by several distinct thermally stimulated processes (KCl [2], CdF_2 [3, 4], NaCl [5]), of which only weak polarisation caused by defect-impurity complex reorientation [6] has been identified and theoretically explained. Because of the intricacy of the TSD currents (thermograms) obtained and because of their rather poor reproducibility, little progress has been made in their understanding. It is conjectured that the lack of reproducibility is caused for the most part by insufficient 'definition' of the crystal-surface electrode interface. Thermograms of nearly ideally insulated polar crystals are simple, of excellent reproducibility and theoretically well understood. They

† In part I [1], the polarisation by fields only was basically investigated.

show, besides the complex polarisation peak(s) at low temperatures (LT), a space-charge (SCH) polarisation peak caused by totally blocked mobile point defects (PD-SCH) predicted by theory (cf. for instance [7]), which can be described under these conditions to a good approximation as surface polarisation (SP) [1, 8, 9].

This peak marks the beginning of a perceptible electrolytic bulk conductivity [10, 11]. In the LT region, below the SP peak, the crystals may be described as insulators; at higher temperatures (HT), however, they are definitely conductors, even if poor ones. Without passing a current, no permanent field can be sustained in the crystals. Optical and electrical measurements of CdF₂ crystals, through which an increasing current was passed by means of a less and less efficient insulation and then by more and more effective contacts respectively, showed that the passage of a current is connected with electron injection into the crystal and with Cd colloid formation adjacent to the cathode. These colloids grow in number and size with the quantity of charge passed, and also the area of a HT TSD peak obtained above the PD-SCH peak is increased [12]. This suggests that the former or perhaps all the HT peaks observed are connected with the colloid formation and/or with the discharge of fluorine ions at the anode, which must necessarily take place, too, if a steady current is to pass in the crystal. On the other hand, the appearance of colloids gives a hint of how the mobile point defects arriving in the course of charge transport at the cathode are discharged if the electrodes are not in ideal contact with the crystal surfaces. The injected electrons are captured at the colloids, which function as a kind of reversible inside cathode at which Cd ions are 'segregated'.

In an effort to elucidate the formation of HT peaks and electrode processes, here we attempt to obtain more reproducible thermograms (§ 2). Further, the dependence of the parameters of the HT peaks on the polarisation conditions and charging and discharging currents were obtained (§ 3). Then, in § 4, earlier published and newly obtained TSD data of CdF₂ are compared. Assuming that differences between individual thermograms are caused mainly by the relevant layout of the crystal-electrode interfaces, the theoretically expected peak caused by PD-SCH formation could be identified. On the other hand, the connection between the layout of the interfaces, electron injection and the observed HT peaks could be corroborated. Finally, in § 5 the mechanisms that possibly cause the HT peaks are discussed.

2. Experimental details

Details concerning the growth of the investigated crystals as well as the technique of TSD measurement are described or quoted in part I [1]. Only a few especially relevant procedures and circumstances are therefore mentioned here.

2.1. Crystal samples

An important requirement of any TSD measurement is a well defined initial state of polarisation. Therefore, crystals with zero polarisation are needed. This can be realised, for instance, by employing in every measurement a 'fresh' crystal which has not been exposed previously to any electrical field. However, this is extremely laborious. Another possibility is to discharge the crystals before measurement. To investigate this possibility, results obtained with fresh crystals were compared with those obtained with crystals that were discharged by shorting them at 500 K until the discharge current I_d was reduced to several 10^{-14} A at 200 K. It is to be noted that the current obtained when fresh crystals

Table 1. Dependence of $(Q/SV)_\infty$ of the first HT peak on various experimental conditions: $T_p = 298$ K and $T_0 = 200$ K.

Crystal material	V_p (V)	t_p (min)	b_{cool} (K s ⁻¹)	b (K s ⁻¹)	$(Q/SV)_\infty$ (10 ⁻⁶ C cm ⁻² V ⁻¹)	
Fresh, undoped	2	10	0.04	0.058	0.39	
	5	5	0.05	0.084	0.51	
	6	20	0.05	0.085	0.42	
	74	5	0.05	0.116	0.53	
	110	10	0.33	0.085	0.39	
average					0.448 ± 7%	
Discharged, doped (wt% NaF IM)	2.0	6	5	0.05	0.062	0.41
	0.5	48	5	0.08	0.083	0.50
	0.1	28	5	0.08	0.080	0.43
undoped		74	5	0.08	0.116	0.53
average						0.445 ± 7%
Fresh, doped (wt% NaF IM)	0.002	6	5	0.36	0.08	0.40
	0.01	6	5	0.30	0.08	0.43
	0.05	6	5	0.30	0.08	0.38
	0.1	6	5	0.30	0.08	0.45
	0.5	6	5	0.30	0.08	0.42
average						0.417 ± 3%

were shorted with the measuring device was only several 10^{-15} A. The comparison did not yield any systematic difference as far as the first HT peak is concerned (table 1), but showed considerable differences as far as HT peaks 2 and 3 are concerned. Any attempt to achieve a more effective discharge by extension of the period of shorting is not feasible, as demonstrated by the data of table 4. By grinding away 100–200 μm of the crystal surfaces, however, it was possible to reduce I_d below the value of the offset current. It is to be noted that I_d is considerably enhanced by the aliovalent impurity content and by the quantity of charge passed through the crystal.

As far as the aliovalent impurity concentration of the crystals is concerned, it is assumed that it is proportional to the concentration in the melt, c , except at high concentrations.

2.2. Measurements and their evaluation

The main subject of this investigation is the TSD currents $I(t, T)$ caused by the passage of a current—and by the field that is necessarily applied to sustain the current. This current and field and their effects are determined by the polarisation conditions, i.e. by the polarisation voltage V_p , by the polarisation temperature T_p and time t_p , and by the initial polarisation P_0 , which, as mentioned before, is generally considered to be zero. On the other hand, the polarisation depends on the defect concentration and on the constitution of the crystal–electrode interface. The crystal thickness L was about 0.1 cm and the contact surfaces of area S (0.74 cm²) were carefully polished and provided with colloidal graphite layers produced by repeated application of a commercial graphite suspension. Besides the TSD, the currents during polarisation and depolarisation at room temperature (RT) were also obtained.

Individual TSD peaks are characterised by their maximum positions T_{\max} , by their areas per unit surface

$$Q/S = (1/S) \int I dt$$

and by the activation enthalpies of the initial rise U , which in the case of a polarisation by mobile point defects are

$$U = k \partial \ln(IT)/\partial(1/T).$$

Finally the peaks are characterised by their shapes. As long as the polarisation current passing through the crystals is weak, for instance when silicon oil is applied to the crystal surfaces, the thermograms consist of individual peaks. If the polarising current is higher, the peaks become extremely broad and overlap one another (figure 1(a)). It is consequently mostly necessary to decompose the bands to obtain their parameters. Because the theoretical shape of the peaks is not known in the present case, this can be done only tentatively. However, experience has shown that T_{\max} depends only marginally on the method of decomposition and that, in spite of an uncertainty in the obtained Q/S values of $\pm 15\%$, reasonably smooth curves of $Q/S = f(t_p)$ and $f(c)$ are obtained. As far as U is concerned, the only reliable method to obtain its value under the given circumstances is peak cleaning (cf. for instance [3], figures 5 and 6). It was possible to abbreviate this lengthy procedure in this investigation by cooling down the samples to only 200 K. Under these conditions the LT and PD-SCH peaks (which will be referred to as LT peaks for

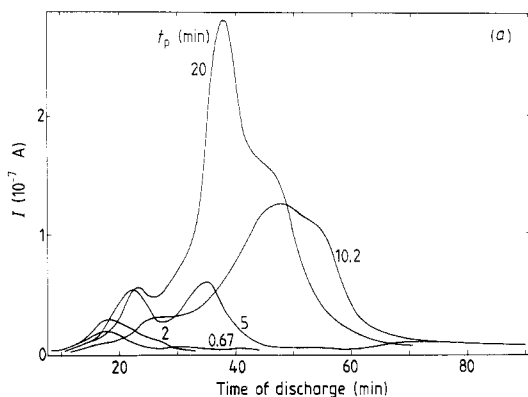
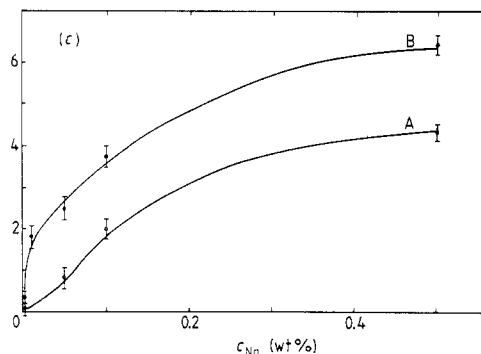
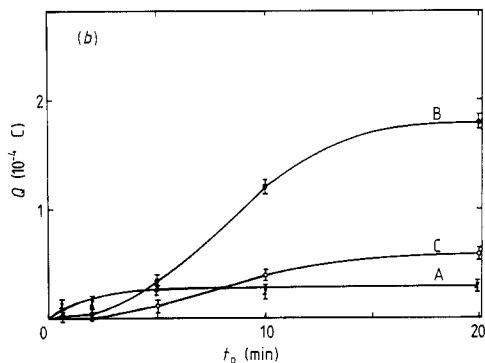


Figure 1. (a) HT TSD current obtained with undoped CdF_2 for various values of t_p : $V_p = 6$ V, $T_p = 298$ K, $T_0 = 200$ K, $b_{\text{cool}} = 0.3$ K s^{-1} and $b = b_{\text{heat}}$ until RT about 0.1 K s^{-1} then about 0.033 K s^{-1} . (b) Peak areas Q as a function of t_p : curve A, first, B, second and C, third HT peaks. (c) Peak areas Q of the second (B) and third (C) HT peaks for $V_p = 6$ V, $T_p = 298$ K, $T_0 = 200$ K and $t_p = 5$ min as a function of the NaF concentration c in the melt.



simplicity) are nearly immediately relaxed when the crystal samples are shorted for the TSD procedure and a 'cleaned' initial rise of the first HT peak is obtained. Repeated measurements have shown that the error in the mean values of U determined in this way does not exceed several per cent. However, U was systematically obtained only for the first peak. As far as peaks 2 and 3 are concerned, only some solitary attempts to estimate its value were made.

3. Experimental results and their analysis

3.1. Thermograms

In general five TSD peaks were obtained with colloidal graphite-contacted crystals between 80 and 450 K. The first is caused by impurity-defect complex reorientation and the second, as will be verified in § 4, by PD-SCH. Hence for undoped crystals the division between LT and HT regions is at about 200 K. To obtain the HT thermograms, these crystals were therefore cooled after polarisation down to only $T_0 = 200$ K. Three TSD peaks, which are referred to as HT peaks numbers 1, 2 and 3, were obtained that way. In figure 1(a) an example of the TSD current of 'fresh' crystals as a function of time, $I = f(t)$, is given. The rate of temperature increase, $b = dT/dt$, was ~ 0.1 K s⁻¹ up to RT and was then decreased to 0.033 K s⁻¹ to prevent I from becoming too high. The peak maxima are at 305–336, 373–390 and 395–410 K. The peaks are so broad that they form a continuous band, called by some authors a dielectric chaos band [5, 13]. The specific peak areas, Q/SV , obtained by decomposition are, after a long enough polarisation, orders of magnitude higher than that obtained with crystals that were 'insulated' or in mere mechanical contact with solid metal electrodes. The mean activation enthalpy U obtained from the initial rise of the first peaks is 0.51 eV. This suggests that the relaxation mechanism of the first peak is connected with migration of mobile point defects.

3.2. Dependence of Q/SV on the polarisation conditions

In figure 1(b) the dependence of the Q values of 'fresh' crystals on t_p obtained by polarising with $V_p = 6$ V at $T_p = RT$ are plotted. The respective growth curves show, first, that after 5–6 min the polarisation that causes peak 1 is reaching a saturation value, whereas peaks 2 and 3 continue to grow. They reach saturation at best after some 20 min, but it probably takes even longer. As peaks 2 and 3 begin to grow noticeably only when peak 1 has attained more than half its final height, their growth mechanism is possibly 'coupled' one way or another to that of peak 1.

As seen from table 1 the saturation values $(Q/SV)_\infty$ of peak 1 are within the limits of experimental accuracy independent of the cooling and heating rates and are reproducible within a few per cent. Furthermore, they are practically independent of the aliovalent impurity concentration, and in the range 2–110 V per 0.1 cm thickness of the crystals they are also independent of V_p .

In figure 1(c) the growth of peaks 2 and 3 with increasing c , that is with increasing point-defect concentration, for $t_p = 5$ min is plotted. These curves show that the peaks increase proportionally to the substitutional built-in impurity concentration. They grow first strictly proportional to c , but then fall increasingly behind as is expected in the case when there is a solubility limit for the impurity. The curves show further that the mechanism of formation of peak 3 is possibly coupled to that of peak 2. The areas of peaks 2 and 3 grow with V_p like those of peak 1, but obviously less than strictly proportional (table 2).

Table 2. Dependence of Q/SV of the HT peaks on the polarisation voltage V_p ; $T_p = 298$ K, $T_0 = 200$ K and $t_p = 5$ min.

Crystal material	V_p/V'_p	t_p (min)	$(1/5) \times Q/Q'$		
			1st	2nd	3rd
0.01 wt% NaF in melt	100:20	5	1.07	0.73	0.93
Undoped	55:11	5	0.85	0.89	0.79

A mathematical analysis of the growth curve of the first peak shows that it approximately follows an exponential law, $(Q/SV)_{\infty}[1 - \exp(-t/\tau)]$, with a relaxation time τ of about 120 s. It is thus orders of magnitude higher than that of the PD-SCH polarisation peak, which builds up at RT practically instantaneously ($\tau \sim 10^{-4}$ s, figure 4 in [1]). If $\tau(T)$ is calculated from $I(T)$ for $t_p = 5$ min, when the overlap of the first two HT peaks was lowest and the error due to the tentative separation of the peaks least, under the supposition of first-order kinetics of the relaxation process, then [13]

$$\ln \tau(T) = \text{constant} + U/kT = \ln \left(\int_{I(T)}^{\infty} I(t') dt' \right) - \ln I(T) \quad (1)$$

about the same τ is obtained for $T = 239$ K. However, it is found that the slope of $\tau(T)$ fits $\exp(-0.51/kT)$ only until T_{\max} ; above it the slope is first increasing, and finally decreasing. This might be caused by insufficient accuracy of the separation procedure, but it possibly suggests that the build-up of polarisation is not a simple first-order kinetic process.

3.3. Currents during charging and discharging, $I_{ch}(t)$ and $I_d(t)$, at RT

These measurements were obtained with discharged crystals through which at least 10^{-4} C cm $^{-2}$ were passed before discharge. The reason for this precaution was the fact that it is only after passage of this quantity that noteworthy colloid formation is observed (see § 5.6) and a reproducible V - A characteristic obtained (see figure 2; [12]). A sequence of I_{ch} and I_d was measured with V_p always pointing in one direction. In principle, curves such as curves A and B in figure 2(a) were obtained. Some current values at $t = 0$ and 12.5 min for different voltages are given in table 3. At the beginning of the charging, $I_{ch}(0)$ is proportional to V_p , that is $I_{ch}/V_p = \text{constant}$. Furthermore, for $V_p = 0.5$ and 2.5 V, I_{ch} and I_d are practically equal for $t = 0$. For $V_p = 10$ V, however, $I_d(0) < I_{ch}(0)$. For $V_p = 0.5$ V, I_d is nearest to the mirror image of I_{ch} . For higher V_p , however, the difference between them increases.

To represent I_d for $V_p = 10$ V by a series of exponentials which would agree within $\pm 3\%$ with the data,

$$I_d = \sum I_n \exp(-t/\tau_n)$$

four relaxation constants were required, 11, 31, 125 and 830 s. The specific charge quantity released,

$$(Q/SV)_d = (1/SV) \int I_d dt$$

was found to depend on the kind of contact realised. It was, however, independent of $V_p < 100$ V for $t_p = 10$ min. With electrodes of graphite values of 0.5 to

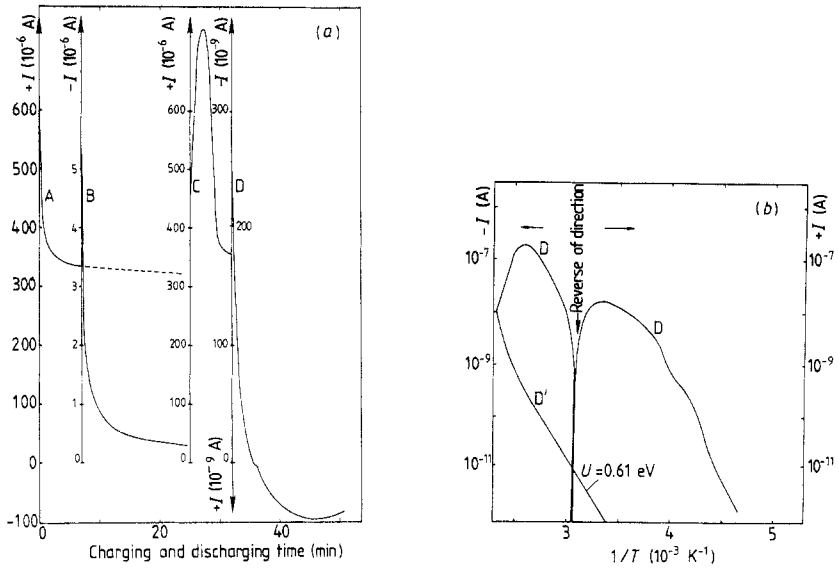


Figure 2. (a) Current during charging and discharging of CdF₂:NaF with a reversal of V_p at RT: (A) $V_p = 75$ V, (B) $V_p = 0$, (C) $V_p = -75$ V and (D) $V_p = 0$. (b) TSD current after periods (A) to (C) obtained during a subsequent heating (D) and cooling (D'). $U = U_m + U_a/2$ (cf. [11]). U_m is activation enthalpy of defect motion and U_a that of impurity-defect association.

$1.2 \times 10^{-6} \text{ C cm}^{-2} \text{ V}^{-1}$, with gold 2.0 to $3.0 \times 10^{-6} \text{ C cm}^{-2} \text{ V}^{-1}$ and with a mere mechanical contact 2.8 to $4.4 \times 10^{-10} \text{ C cm}^{-2} \text{ V}^{-1}$ were obtained.

3.4. Currents during charging and discharging at RT after a reversal of V_p

In a second series of measurements, a sequence of I_{ch} and I_{d} was obtained (figure 2(a)), with alteration of the direction of V_p though, after a first charge (A) and discharge (B) period. When the direction of V_p was then reversed (C), the initial charging current was somewhat lower than $I_{\text{ch}}(0)$ in (A) first, but then rose above this value finally to decay as in (A). In the following discharge (D), $I_{\text{d}}(0)$ was only about 0.0004 of $I_{\text{ch}}(0)$ in (A), whereas in (B) it was about 0.01. After about 3 min I_{d} became zero, finally changing direction. After attaining a maximum, after 13 min, it began to fall again.

For periods (C) and (D) the observed current can be explained by the existence of two current components of opposite sign (cf. [14]). At the beginning of period (C), after only 17 min of discharge, the crystal was not yet completely discharged. Hence at one electrode a surplus and at the other a deficiency of mobile defects still existed, as well as a field in the direction of V_p during period (A). It is compensated ($V_p = 0$) by a field of

Table 3. Currents during charging and discharging, I_{ch} and I_{d} , and their relative decay $I'(t) = I(t)/I(0)$: I (10^{-9} A), V (volts) and t (min).

V_p	$I_{\text{ch}}(0)$	$I_{\text{ch}}(0)/V_p$	$I'_{\text{ch}}(12.5)$	$I_{\text{d}}(0)$	$I'_{\text{d}}(12.5)$
0.5	5.7	11.4	0.021	5.7	0.009
2.5	29.4	11.7	0.090	29.0	0.014
10.0	116.0	11.6	0.660	>60.0	<0.018

opposite direction in the bulk. When the reversed field is then applied, the field strength in the bulk becomes higher than in period (A) and a higher current component in the direction of V_p is obtained. At the same time, however, a notable short-lived current component of opposite sign flows at the electrodes because of the high defect concentration and depletion, respectively, at the electrodes and because field drift and diffusion have the same directions.

If after polarisation with the reversed field (C) the crystal was cooled down and a TSD obtained, two peaks or rather bands of opposite sign were obtained (figure 2(b)). As soon as 400 K was reached, the sample was cooled down again. After a while the abrupt decay of the current became exponential in $1/T$ with a slope similar to that of the initial rise. This suggests that the peaks are caused, in principle, by the same kind of charge carriers but by different driving forces of opposite directions. This situation indicates that there exist two different polarisation regions as suggested above. The fact that the change of sign of the TSD current is extremely abrupt further suggests that the two polarisation components are not too different in magnitude.

3.5. Long-run discharge currents

A considerably high and persistent depolarisation current is obtained with doped crystals and with higher values of V_p and t_p (table 4). After 32 h at RT I_d fell by three orders of magnitude. But still, by increasing the temperature after more than 7 days to 473 K, the discharge current rose to somewhat above the original value of several microamps. At this time the totally released charge already surpassed Q/S of the first peak by two orders of magnitude. The increase of the discharge current, which was caused by the temperature rise, is proportional to a Boltzmann factor with $U = 0.47$ eV. This is compatible with an activation enthalpy of about 0.51 eV if the fact is taken into account that also during the temperature change a certain quantity of a charge was released. This and other such observations suggest that all the HT peaks are caused immediately by drifting mobile point defects.

The crystal was finally slowly cooled down after the described procedure to reach RT after 4 days. At RT the discharge current was then two orders of magnitude lower than before the temperature rise, but still orders above the zero line of fresh crystals.

Table 4. Long-run discharge current of 0.1 wt% NaF-doped CdF_2 ; $V_p = 100$ V, $t_p = 30$ min and $T_p = 298$ K.

Time of discharge	T (K)	I_d (t)	Released charge (C)
0	398	3.0×10^{-6}	
5 s		1.4×10^{-6}	1.2×10^{-5}
5 min		1.4×10^{-7}	4.7×10^{-4}
8 h		1.7×10^{-8}	9.4×10^{-4}
24 h		5.3×10^{-9}	1.3×10^{-3}
6 d		5.2×10^{-9}	3.5×10^{-3}
Heating			
0	473	4.0×10^{-6}	3.5×10^{-3}
3.5 h	423	5.6×10^{-8}	6.6×10^{-3}
21 h	363	2.5×10^{-9}	6.8×10^{-3}
3 d	273	3.0×10^{-11}	6.9×10^{-3}

4. Comparison of published and present CdF₂ TSD data

If the present work and individual measurements previously published are compared, a confusing diversity of peak positions and magnitudes is found (table 5). However, the various data were obtained with different arrangements of the crystal-electrode interfaces and with different cooling temperatures T_0 . When the data are arranged starting from crystals insulated with $2 \times 470 \mu\text{m}$ of sapphire, a nearly ideal insulation, to thinner, less effective insulations, and then to improving conductive electrodes, systematic trends do emerge. An attempt will be made to show that these trends can be explained, at least qualitatively, by the actual crystal-electrode layout. The data quoted in the discussion are found in the lines (1–12) in table 5.

Besides the data of table 5, some data obtained with Teflon-insulated crystals have been published [8]. However, because neither the values of δ , Q/SV nor the impurity concentrations were given, comparison with the rest is difficult.

Table 5. Survey of TSD peaks obtained above the complex peak(s), up to the present day.

	<i>c</i> (mol% NaF)	<i>T</i> _{max} (K)	<i>U</i> (eV)	<i>Q/SV</i> (C cm ⁻² V ⁻¹)	<i>I</i> _σ (300 K)	Reference
1 $2 \times 470 \mu\text{m}$ sapphire, <i>T</i> ₀ = 73 K	0.05	198–203	0.64–0.74 ^a	3.6×10^{-12}	$<1 \times 10^{-15}$	[11], <i>U</i> _σ = 0.69 eV
2	undoped	204–219	0.65–0.74 ^a	3.6×10^{-12}		
3 $2 \times 95 \mu\text{m}$ sapphire, <i>T</i> ₀ = 80 K ^b	0.05	198 270–278	0.67 ^a —	1.9×10^{-12} 0.4×10^{-12}	1×10^{-13}	<i>U</i> _σ = 0.69 eV
4 $2 \times 6 \mu\text{m}$ oil, <i>T</i> ₀ = 73 K	undoped	194–207 ^c	0.50–0.54	$1.4\text{--}5 \times 10^{-11}$	2×10^{-8}	[1]
5	0.1	160–166 198 236	0.49	3.6×10^{-11} 1.0×10^{-11} 6.7×10^{-11}		
6	0.5	135–137	— ^d	$2\text{--}4 \times 10^{-11}$		
7 Graph. electr., <i>T</i> ₀ = 90 K	undoped	197 ^e	0.51	4.4×10^{-11}		[4], <i>T</i> < 320 K
8	0.5 ^f NaF	140 254	0.34 ^d 0.51	4.7×10^{-11} 1.7×10^{-10}		
9	0.5 ^f YF ₃	177 230	0.36 0.33	2.2×10^{-13} 5.1×10^{-12}		
10 Graph. electr., <i>T</i> ₀ = 200 K	undoped	328 383	0.48 0.81 ^g	8.8×10^{-7} 2.6×10^{-6}	1.5×10^{-8}	[3], <i>T</i> < 380 K
11	0.5 ^f NaF	260 349	0.48 0.81 ^g	2.7×10^{-6} 2.1×10^{-6}		
12 Graph. electr., <i>T</i> ₀ = 200 K	undoped	305–336 373–390 395–410	0.51			Present meas.

^a In this case $U = U_m + U_a/2$ [11].

^b Data from [24].

^c Only the sp peak was measured.

^d Peak overlapping with the complex peak.

^e *T*_p = 193 K. For the effect see [22].

^f Wt% in the melt.

^g For possible reason of $U > U_m$ see [10].

4.1. Nearly ideally insulated crystals

In this case, up to a temperature of 430 K, when the insulating power of sapphire begins to decrease, only LT peaks, that is a complex reorientation peak at 95 K with NaF-doped CdF₂ crystals [4, 8, 15] and an SP peak caused by mobile point defects, are obtained (lines 1 and 2). The parameters of the SP peak are in excellent agreement with theoretical expectations [11], and the efficiency of the insulation, which is a precondition for this agreement, is confirmed by the fact that no current that exceeds the 'leakage or background current' of the measuring device ($<10^{-15}$ A) is observed besides the TSD current peaks. It is to be noted that with the Teflon-insulated crystals, which were doped with various aliovalent impurities too, always only a complex and an SP peak were obtained [8].

4.2. Incompletely insulated crystals

TSD measurements between about 70 and 300 K with a thinner, less efficient insulation show, besides the LT peaks, one or two HT peaks above the SP peak (lines 3 and 5). The increasing steady-state current passing in the crystals, I_σ , demonstrates the decreasing insulating power of the arrangements. Correlated with this is an increase of HT peaks (see also [12]). With decreasing insulation thickness δ and increasing I_σ , some of the parameters of the SP peak show an increasing deviation from the values predicted by theory. The value of U obtained from the initial rise equals that of the conductivity, σ , i.e. $U = 0.51$ eV = U_m , the enthalpy of activation of defect motion. If an attempt is made to find the best fit of the data by a first-order kinetic equation, again $U = 0.51$ eV is obtained. However, a fit can be attained only an order of magnitude below the maximum TSD currents. In the case of ideally insulated crystals, the best fit stretched over nearly three orders of magnitude. Next Q/SV drops increasingly behind the increase, which should result from decreasing δ (equation (2.12) of [9]). This is no doubt a consequence of the increasing voltage drop, ΔV , caused by I_σ in the bulk and probably also by polarisation connected with the HT peaks. For $\delta = 6$ μm (line 4), for instance, instead of the theoretical expected value of 6.56×10^{-10} C cm⁻² V⁻¹, only 5.0×10^{-11} C cm⁻² V⁻¹ is obtained.

According to the SP model, T_{\max} should shift further towards higher temperatures with decreasing δ [9], i.e.,

$$T_{\max} \approx [(bU/k)\tau(T_{\max})]^{1/2} = \{(bU/k)[\epsilon_0(2\delta\epsilon + L\epsilon_i)/2\delta]\sigma(T_{\max})^{-1}\}^{1/2}. \quad (2)$$

To estimate the effect of decreasing δ on T_{\max} , equation (2) is rearranged in terms of capacity C and resistance $R(T)$ as

$$\tau(T_{\max}) = [\epsilon_0(\epsilon_i/2\delta + \epsilon/L)S][\sigma(T_{\max})^{-1}(L/S)] = CR(T_{\max}). \quad (3)$$

A decrease in δ will change the value of both. Because Q/S is decreased, C appears smaller: $C = Q/V_p$. Furthermore, a decreased Q necessarily means a proportionally decreased TSD current I so that R appears higher: $R = V_p/I$. Consequently T_{\max} stays practically the same (cf. lines 2, 4 and 7). A higher σ caused by an increased c , on the other hand, should shift T_{\max} under otherwise unchanged conditions to lower temperatures, as in fact it does (see lines 4, 5, 6 and 8).

The surface polarisation is caused in reality by the space charge of totally blocked point defects under conditions which allow an approximation of SCH formation by the SP model [1]. These conditions are a thick and powerful enough insulation. In the case

when δ was only a few micrometres, such conditions certainly were not realised. Still, even then, space-charge formation by totally blocked point defects (PD-SCH) according to the accepted SCH theory [7] should take place. Inspection of the general solution of SCH formation [16] shows that the dependence on σ , of the initial rise and of T_{\max} should in fact last. Only Q/SV , the shape and τ should change, and then only gradually. It may thus be said that incompletely insulated crystals also show at LT above the complex peak a PD-SCH peak, which is, at least qualitatively, in agreement with the theoretical expectations and again marks the beginning of conductivity.

4.3. Contacted crystals

Earlier data obtained with colloidal graphite electrodes between 90 and 320 K show, above the complex peak, a second peak, at about 197 K with an undoped crystal and at 140 K with a 0.5 wt% NaF-doped crystal (lines 7 and 8). In the case of the undoped crystal, $U = 0.51 \text{ eV} = U_m$ was obtained. For the doped crystal, U was only 0.34 eV, but the peak is overlapping with the high-temperature tail of the complex peak (cf. § 2.7.2 of [9]). Hence, obviously, a too low value of U was obtained. That the enthalpy of activation of the discussed peak is really identical with U_m is clearly confirmed from the data of the YF_3 -doped crystal (line 9). Here $U = 0.36 \text{ eV}$ is, within error limits, equal to the enthalpy of activation of σ of $\text{CdF}_2:\text{YF}_3$ (0.33 eV, [3]). Finally an estimation of τ from the left side of equation (2) yields $\sim 10^{-4} \text{ s}$ at 300 K, as is obtained for the SP peak at this temperature. All these facts again point to PD-SCH as the cause of the discussed peaks.

From the above it follows that the first HT peaks of $\text{CdF}_2:\text{NaF}$ and $\text{CdF}_2:\text{YF}_3$ are the peaks at 254 and 230 K respectively. The fact that U is again similar to U_m , that is 0.51 and 0.33 eV respectively (lines 8 and 9), suggests that the relaxation of the first HT peak is again connected with transport of point defects. On the other hand, the different T_{\max} is not the only dissimilarity between the HT and PD-SCH peaks. Thus the position of a PD-SCH peak does not depend on T_p whereas that of the first HT peak is shifted, for instance, from 254 to 203 K (table 1, [4]) when the crystal is polarised at 193 K instead of at 300 K. Finally the relaxation times are different by orders of magnitude, 120 s (§ 3.2) and $\sim 10^{-4} \text{ s}$ (figure 4 of [1]) at RT, and so are the peak areas.

The first TSD measurements obtained with CdF_2 provided with colloidal graphite contacts, which covered the temperature range from 200 to 400 K, show only HT peaks (lines 10 and 11). A PD-SCH peak could not be obtained with $T_0 = 200 \text{ K}$ because the point defects are already mobile at this temperature, as explained in § 2.2. The thermograms of both undoped and NaF-doped crystals show first HT peaks with $U = 0.48 \text{ eV}$. The value of U was obtained from $\ln I$. Evaluation of $\ln(IT)$ again yields about 0.51 eV. The position obtained with the doped crystal is about the same as in the above-quoted measurements. The position of the first HT peak obtained with the undoped crystal (328 K) shows that this peak could not be observed in the measurements (line 7), because these did not extend beyond some 300–320 K.

As far as the new measurements are concerned, the positions of HT peaks 1 and 2 and the value of U of the first peak from before are confirmed in principle; the third peak, which was obtained in addition, appears at temperatures that were not covered by any of the preceding measurements.

4.4. Further peaks: shoulder on the LT side of HT peak 1

Besides the three named HT peaks, some further peaks were obtained in the HT region.

The thermograms of undoped crystals occasionally show a pronounced shoulder on the LT side of HT peak 1 and so do the thermograms obtained with YF_3 -doped crystals (figures 4(b) and (c) of [3]). If the shoulders were separated under the assumption that the activation enthalpies of HT peak 1 are 0.49 and 0.30 eV respectively, small peaks with $U = 0.3$ and 0.46 eV respectively were obtained (see figure 5 of [3]). This suggests that the appearance of these peaks is caused by complementary point defects, i.e. by interstitial fluorine and anion vacancies respectively.

This notion seems plausible. When an undoped crystal is polarised and anion vacancies are accumulated at the cathode, they are necessarily depleted at the same time at the anode. This is caused by transport of fluorine ions towards the anode. In due course, the arriving fluorine anions must end up in interstitial positions, that is, as complementary defects. This probably then leads to formation of neutral fluorine and to emission of electrons necessary to sustain I_σ . In YF_3 -doped crystals again, because of depletion of interstitial fluorine at the cathode, anion vacancies should be formed. It is to be noted, however, that a strong enough shoulder should be obtained only when the crystal is excessively polarised. The above interpretation of the shoulders is strongly supported by dielectric loss data of undoped crystals attributed to PD-SCH formation. The relaxation clearly shows two maxima with $U = 0.51$ and 0.33 eV respectively (figures 3 and 4 of [1]).

4.5. Reversed peaks: initial non-zero polarisation

In some measurements, reversed peaks, that is peaks which have the same direction as the polarisation current, were obtained (see for instance figures 1 and 3 of [4]). As demonstrated in § 3.4, reversed currents are the result of the existence of a non-zero initial polarisation opposed to the direction of V_p . That is to say, the crystals were not sufficiently discharged before measurement.

5. Discussion of the available data

When discussing the HT TSD data, three 'peculiarities' compared with the usual TSD have to be taken into account. First, the extremely high quantities of released charge cannot really accumulate on the electrodes because, at the applied voltages, this would cause already unrealistic fields of the order of 10^8 V cm^{-1} at the electrode surfaces. As a matter of fact, from potential distribution measurements, fields many orders of magnitude weaker are obtained (see § 5.3). Secondly, the crystals are, in the HT region, conductors and consequently no polarisation field can exist in the shorted crystals at high temperatures. Any such field would inevitably be compensated by mobile point defects. Consequently the HT peaks cannot be caused immediately by relaxation of dielectric polarisation. In fact, after the PD-SCH peak, the depolarisation current drops in general until the zero line before it begins to rise again towards the maximum of HT peak 1 (figure 3 of [17], line 10, figure 4(b) of [3]). This shows that the crystals were totally depolarised and that the driving forces which cause the HT peaks become effective or come into being only at appropriately high temperatures. Also peaks 2 and/or 3 are most probably (cf. for instance § 3.5) caused immediately by transport of point defects. Finally, the transformation of ionic charge carriers into electrons and vice versa, which is a precondition for the passage of a steady current through a crystal, is connected with electron injection and colloid formation at the cathode, a notion which stood the test in explaining the differences between the various known TSD data in § 4.

5.1. The build-up and relaxation of 'polarisation' at RT

It is generally assumed (superposition law) and has sometimes been experimentally confirmed [18] that

$$I_d = -(I_{ch} - I_\infty)$$

where I_∞ is the value of the ultimate steady current. This suggests that the difference between I_{ch} and I_d should yield the current passing through the crystal, I_σ . It is found from the data of § 3.3 that, in the present case for $V_p = 2.5$ and 10 V initially, in the first 10–20 s this difference drops from an initial value of the order of I_∞ down to zero. The parameters of this fast initial decay are poorly reproducible, but the decay itself is no doubt real. Then the difference increases again within 2–6 min to a value that is approximately constant, before the long-lived component(s) of the polarisation make themselves felt. If it were assumed that I_σ is equal to I_∞ from the beginning, the superposition law would be violated. I_d would then be higher than $I_{ch} - I_\infty$. At $t = 0$ the difference would be zero, but after 10–20 s it would become about equal to I_∞ , to decay then completely within 5–6 min. It is difficult to imagine a process that would cause such a strange deviation from the superposition law. Furthermore, it follows from §§ 3.2 and 3.3 that $(Q/SV)_d$ is practically equal to the specific peak area $(Q/SV)_\infty$ of peak 1, and so are the relaxation times of this peak (120 s) and of the dominant component of I_d (125 s). These facts show that it is basically the process which causes HT peak 1 that determines I_d . Consequently the build-up of the relevant polarisation at RT is at least proportional to it—which justifies the above procedure of decomposition of I_{ch} .

The difference between I_{ch} and I_d includes of course also contributions to I_{ch} of all the other polarisation processes according to their relaxation times at RT. The contribution of the PD-SCH with $\tau \sim 10^{-4}$ s, though, cannot be detected with the measuring device used because its time lag is several seconds. The build-up of the PD-SCH is nevertheless evident from AC measurements (figures 3 and 4 of [1]) and from TSD thermograms quoted in table 5 (lines 7–9). The total charge and τ of the fast initial component are of the order of 10^{-8} C cm⁻² V⁻¹ and 11–31 s respectively. It is conjectured from these values that it is perhaps caused by the assumed (§ 4.4) complementary defect accumulation. The weak component with $\tau = 830$ s finally might be connected with the formation of peaks 2 and 3.

5.2. Peak 1: relaxation of the inside cathode polarisation

The suggested decomposition of I_{ch} into basically a charging component $-I_d$ and I_σ finds a plausible explanation in colloid formation. The instantaneous build-up of the PD-SCH should cause an immediate increase of the field strength at the cathode from $V_p/L = 50$ and 100 to several 10^3 V cm⁻¹ and, hence, electron injection. It is obvious that the majority of electrons should be captured by colloids, which are thus charged. Their electronic charge, however, will be compensated by accumulation of mobile point defects in the vicinity of the colloids, with the formation of a kind of micro-SCH. It is expected that the resulting fields at the colloid surfaces should become very high, especially because of the small colloid radii. This should then cause first tunnelling or diffusion [19] of electrons to more distant colloids and secondly segregation of neighbouring Cd ions at the colloids, that is 'discharge' of point defects and I_σ . The rates of these processes tend in due course towards equilibrium with electron injection: the charging of the colloids then comes to an end and I_{ch} becomes constant, i.e. equal to I_∞ . These deliberations suggest that peak 1 reflects the inside cathode polarisation.

If I_d is basically equal to $-(I_{ch} - I_\sigma)$, it is expected that the build-up and relaxation of peak 1 are caused by more or less similar mechanisms. As long as V_p is on, electrons and point defects are driven into the 'colloid cloud' and micro-SCHs should be formed, beginning from the surface. If the crystal is then shorted, the direction of the field is changed in the bulk of the crystal, but near the electrodes it is preserved. Consequently, at the inside fringes of the colloid cloud, an outwards migration of electrons and point defects is then favoured by the field. In this way a layer-by-layer relaxation should take place and practically the same extremely long relaxation times and the same activation enthalpies for the build-up and relaxation are obtained.

5.3. The steady-state polarisation

The assumed micro-SCHs should each form a kind of dipole in the crystal, pointing in the field direction. Because of this dipole character, they should cause only a modest potential drop. This notion is in agreement with the potential distribution in the crystal. From $V(x)$ obtained with $V_p = 6$ V [20], a charge density value of several 10^{-11} C cm $^{-2}$ at the electrodes and a depth of a SCH region of about 20 μ m are calculated, whereas from I_d a charge density of $(Q/S)_d = 3$ to 7×10^{-6} C cm $^{-2}$ caused by point-defect transport is obtained (§ 3.2). This seems to be a contradiction. However, according to the assumption of the preceding paragraph the point defects only 'compensate' the injected electronic charge, so the apparent discrepancy is more likely an agreement. $(Q/S)_d$ is caused by the charge transport connected with the formation of 'dipoles'; the former charge density, however, is caused by the dipole field.

It is to be noted that $V(x)$ can hardly be explained by the existence of PD-SCH, because this SCH extends, judging from numerical calculations [21], only a few micrometres deep. Finally, there exists clear evidence that the decay of I_{ch} cannot be caused by the build-up of dielectric polarisation. If the decay were caused by a potential drop caused by a space charge, this would require a reduction of the initial field strength in the bulk to about 1% of V_p/L . The potential distribution data, however, show that the field strength in the bulk is diminished only to about $0.86 V_p/L$.

5.4. The parameters of the peak

The polarisation process is, as follows from the preceding paragraphs, extremely complicated. Compared with this, far too few experimental data are available to trace out details. Consequently, the following suggestions are but speculative.

(i) *The activation enthalpy.* Electron injection and transport by tunnelling depend on the field conditions and only the transport of point defects is enhanced by an increasing T proportionally to a Boltzmann factor with U_m .

(ii) *The relaxation time.* Its extremely high value seems to be explained by the fact that, on the one hand, a multitude of electron jumps is necessary to charge or discharge successively all the colloids and, on the other, any change of position of an electron again requires a multitude of point-defect jumps to be counterbalanced.

(iii) *The shift of T_{max} with T_p (table 1, lines 2-4; [4]).* It was concluded in § 5.2 that the charge is built up successively from the surface. As the diffusion coefficient of the point defects is increasing according to the Nernst-Einstein relation more quickly with increasing T than their mobility, the depth of the charge distribution depends on T and consequently so does the peak position [22].

(iv) *The peak areas.* The PD-SCH, the voltage drop in the SCH free bulk, ΔV , and the micro-SCH at the colloids are vaguely proportional to V_p . Consequently $Q/SV = \text{constant}$ is obtained (table 1). An increased c means an increased number of colloids because already in the first stage of their formation when electrons are trapped by anion vacancies (cf. § 5.6) the concentration of the latter is increased. It is conjectured that the rate of electron injection is then increased proportionally to the increased number of colloids even if V_p stays the same. Possibly the decrease of ΔV caused by the increased σ then compensates an increase of the voltage drop caused by the colloid cloud so that Q/S is independent of c (table 1).

5.5. The second and third HT peaks

It has been stated already that the colloids form a kind of reversible inside cathode. Besides that, most probably neutral fluorine is formed at the anode (cf. § 4.4). The crystal should therefore comprise a kind of solid-state battery, the internal resistance of which depends on σ . Consequently, even after complete relaxation of any polarisation, a weak current is sustained by this battery in the direction of the discharging current. As the internal resistance of this battery is exponentially decreasing with $1/T$, the current is increasing accordingly.

In agreement with this notion, after some time a constant discharge current over several days was obtained at constant RT (table 4). Furthermore, the areas of HT peaks 2 and 3 increase with the quantity of charge passed (figure 1(b)) and at a fixed value of t_p with the impurity concentration (figure 1(c)), that is with the mass of the colloids. Before the colloids begin or continue to grow, they must be charged. Consequently, the growth of peak 2 is coupled to that of peak 1. Finally the growth of peak 3 lags behind that of peak 2. This shows that a certain quantity of fluorine must arrive at the anode before it begins to take up interstitial positions, etc.

5.6. Addendum

5.6.1. *The colloid formation process.* Measurements of the optical density D of crystals through which charge Q/S was passed show that basically [23]

$$D \propto D_0 + \text{constant} \times \ln(Q/S).$$

Until a few $10^{-4} \text{ C cm}^{-2}$ the density is equal to D_0 , which is constant or marginally increasing. Then D begins to increase substantially. It is suggested that electrons are first captured only by anion vacancies (see [19]). This does not increase the extinction much. Attempts to produce colour centres in CdF_2 have so far not been very successful. This might be interpreted as lack of stability, which should favour, via agglomeration, the formation of colloids. It is of interest that in alkali halides such an effect is known. Above $10^{-4} \text{ C cm}^{-2}$ the growth of colloids then prevails and leads to increasing extinction.

5.6.2. *Perfectly contacted crystals.* Electrodes may show basically two kinds of shortcomings: they may be non-reversible or inert and their fit with the crystal surfaces may be incomplete. It is expected that ideally fitting reversible cathodes should prevent the formation of an inside cathode. The fact that with such cathodes a linear $V-A$ characteristic through zero was obtained [20] strongly supports this view.

6. Conclusions

In the first place it was possible to obtain reproducible HT thermograms and, based on the actual layout of the crystal–surface electrode interfaces, the earlier published and present data of CdF₂ could be correlated. Because of the very complicated situation, the discussion was necessarily speculative in many points. Nevertheless, the basic processes which cause the HT peaks can be named. The obtained TSD, charging and discharging currents are caused by three kinds of processes: (i) by the known reorientation of dipolar defect impurity complexes [6]; (ii) by two distinct processes connected with blocking and insufficiently fitting electrodes, namely formation of a space charge by accumulated and depleted point defects at the surfaces (see for instance [7]) and polarisation of the inside cathode [12] formed and charged by electron injection, caused by the enhanced field of the point-defect space charge; (iii) by an electrochemical potential brought about by Cd and fluorine segregated in the course of charge transport below the contact surfaces. Unnoticed variations of the actual layout of the crystal–electrode interfaces and the interdependence of these processes bring about what appeared to many authors, for instance [5, 13], to be dielectric chaos.

References

- [1] Kessler A 1981 *J. Phys. C: Solid State Phys.* **14** 4357
- [2] Bucci C and Riva S 1965 *J. Phys. Chem. Solids* **26** 363
- [3] Kessler A and Caffyn J E 1972 *J. Phys. C: Solid State Phys.* **5** 1134
- [4] Kessler A 1973 *J. Phys. C: Solid State Phys.* **6** 1594
- [5] McKeever S W S and Hughes D M 1978 *J. Phys. Chem. Solids* **39** 211
- [6] Crawford J H Jr and Slifkin M L (ed.) 1972 *General and Ionic Crystals; Point Defects in Solids* vol 1 (New York: Plenum)
- [7] Lidiard A B 1957 *Encyclopedia of Physics* XX/II (Berlin: Springer)
- [8] Kunze I and Müller P 1972 *Phys. Status Solidi a* **13** 197
- [9] Kessler A 1985 *Phys. Status Solidi a* **90** 715
- [10] Kessler A 1980 *J. Phys. Chem. Solids* **41** 793
- [11] Kessler A and Appel W 1983 *Radiat. Eff.* **75** 85
- [12] Kessler A 1980 *J. Physique Coll. Suppl.* **41** C6 492
- [13] Bucci C and Fieschi R 1966 *Phys. Rev.* **148** 816
- [14] Harris L B 1971 *Phys. Status Solidi b* **48** 663
- [15] Kessler A and Pflüger R 1978 *J. Phys. C: Solid State Phys.* **11** 3375
- [16] Jaffe G 1933 *Ann. Phys., Lpz.* **16** 217
- [17] Kessler A and Pflüger R 1977 *J. Electrostat.* **3** 93
- [18] Sutter P H and Nowick A S 1963 *J. Appl. Phys.* **34** 734
- [19] Teltow J 1973 *Cryst. Latt. Defects* **4** 197
- [20] Krok K, Bogusz W, Jarosz J and Jakubowski W 1978 *Phys. Status Solidi a* **47** K103
- [21] Macdonald J R 1954 *J. Chem. Phys.* **22** 1317
- [22] Kessler A 1976 *J. Electrochem. Soc.* **123** 1236
- [23] Weisshaar G 1982 *Diploma Thesis* University of Stuttgart
- [24] Appel W 1981 *Diploma Thesis* University of Stuttgart